

Performance of Climate Projections for Yukon and Adjacent Northwest Territories, 1991–2020

Astrid Schetselaar,^{1,2} Trevor Andersen¹ and Christopher R. Burn¹

(Received 29 October 2022; accepted in revised form 14 February 2023)

ABSTRACT. Permafrost foundation design recognizes the impact of climate change on soil bearing capacity, as described in Canadian guideline CSA PLUS 4011:19. There is, however, no guidance as to the climate scenarios most prudent to adopt for such design. We have compared climate change scenarios outlined in 2003 for the design of the proposed Mackenzie Gas Project (MGP) with climate data for 1991–2020 to determine the projections most representative of what did, in fact, occur. In Canada, the greatest change in climate during the last 50 years has been measured in the western Arctic, where fluctuations in annual air temperatures are regionally consistent. In this region, the rate of change in annual mean air temperature for 1971–2020 has ranged from 0.77 °C decade⁻¹ at Inuvik, NT, to 0.30 °C decade⁻¹ at Komakuk Beach, YT, with warming concentrated in winter. No statistically significant trends in total annual precipitation have been observed and these records are poorly correlated within the region. In 2003, 29 climate projections from seven global climate models were examined for the MGP and, in 2005, for research regarding forest fires in Yukon. The observed climate warming in Yukon and adjacent Northwest Territories during 1991–2020 was close to the upper projections for mean annual and winter air temperature. For example, at Inuvik the 2.3 °C increase observed in mean annual air temperature between 1961–90 and 1991–2020, exceeds the median projection for change by 2010–39 of +1.6 °C and approaches the upper value of +2.4 °C. No consistency between observed and projected precipitation has been determined. These results indicate that, when required, future projections of temperature in northwest Canada may prudently adopt higher or more extreme scenarios because they have been the most realistic to date. They imply that near-surface permafrost may soon become unsustainable in southern parts of the region and so site investigations to locate thaw-stable soils will likely be cost effective for new projects.

Key words: climate change; Yukon; Mackenzie Valley; climate scenarios; temperature; precipitation; engineering design; infrastructure foundations

¹ Department of Geography and Environmental Studies, Carleton University, 1125 Colonel By Drive, Ottawa, Ontario K1S 5B6, Canada

² Corresponding author: astridschetselaar@cmail.carleton.ca

INTRODUCTION

The Arctic as a whole is warming more rapidly than the rest of the planet (Zhang et al., 2019; Rantanen et al., 2022), and the western Canadian Arctic experienced the greatest warming of all regions in the country during 1946–2012 (Fig. 2 in Vincent et al., 2015). Projections of future climate depend on the simulation of greenhouse gas emissions that are used, but all indicate continued warming over the next two decades at least, with Arctic warming exceeding the global average (Bush and Lemmen, 2019; IPCC, 2021a, Section 4.5.1.1). Long-term trends in precipitation are not as clear, but rainfall is expected to increase as temperatures rise and snow is replaced by rain in spring and early autumn (Vincent et al., 2015; Bintanja and Andry, 2017). The IPCC's Sixth Assessment projects increases in precipitation as well as temperature “everywhere in Canada over the 21st century” (IPCC, 2021a: Atlas 9.4).

Prior to the environmental assessment of the Mackenzie Gas Project (2004–10), a group was assembled to provide scenarios of climate change during the proposed service life of the pipeline and its associated facilities (~2010–40) (Burn, 2003). The group contained representatives from industry, non-governmental organizations, regulatory agencies, academia, and federal science agencies. The group met in October 2003 and achieved consensus on climate change scenarios to be used in the environmental assessment, in order to consider the impacts of climate change on the project. A report from the meeting was promptly published and a conference paper disseminated the results more widely (Burn, 2003; Burn et al., 2004). These publications presented climate projections for Mackenzie Valley. Subsequently, a similar selection was made for Yukon, during research on forest fire incidence and intensity (McCoy and Burn, 2005).

There has been considerable interest in the ecological consequences of climate change in northern Canada (e.g., Fraser et al., 2014; Wilcox et al., 2019) and of the effects climate change has induced in permafrost terrain (e.g., Kokelj et al., 2017; Burn et al., 2021a). Similarly, the potential degradation of carbon currently stored in permafrost and its release as CO₂ or CH₄ has stimulated substantial research (e.g., Schuur et al., 2015; Miner et al., 2022). Of immediate financial consequence, however, are the effects of permafrost degradation beneath surface infrastructure (Melvin et al., 2017; Hjort et al., 2018, 2022). Projections of such effects depend on the scenario that is used to outline the scale of climate change to be expected. Owners of infrastructure require adequate awareness of potential climate change that may occur over the intended service life of their projects in order to: (1) assess the extent of capital investment that is required in the foundation during initial construction, (2) estimate the degree of rehabilitation and maintenance that will be required during project life, and (3) settle on a balance between these costs that adequately manages the risks associated with permafrost degradation.

The Canadian Standards Association (2019) has published a technical guideline “Infrastructure in permafrost: A guideline for climate change adaptation” to outline a process whereby climate change may be assessed in foundation design. A key component of the process is determination of the risk that permafrost thaw due to climate change poses to infrastructure and contingent numerical modelling to specify required cooling of soils to maintain foundation integrity. Case studies describing application of the process for the design of the Inuvik Regional Health Centre, NT, and reclamation of several DEW Line sites have been presented by Hayley and Horne (2008). The guideline relies on climate-change projections published by the IPCC, but it does not provide categorical criteria to enable a developer to select a likely future climate for planning purposes. This is primarily because future emissions pathways are unknown.

Nevertheless, climate-change scenarios driven by various emissions pathways were published over 20 years ago by the IPCC (2000) in its Third Scientific Assessment and were assembled for Canada in the Canadian Climate Impacts and Scenarios project (CCIS) at the University of Victoria. Examination of these projections with respect to the accumulated record may provide evidence to guide developers regarding a choice of future scenario (e.g., Bonsal and Kochtubajda, 2009). The purpose of this paper is to examine the projections available in 2003 for Yukon and Mackenzie Valley (Fig. 1) and compare them with the subsequent record. The intention is to determine if the scenarios underestimated, overestimated, or were consistent with recent observations. The scenarios relate to air temperature and precipitation on annual and seasonal bases, projecting changes in these indices with respect to baseline conditions in 1961–90. In 2003, scenarios formulated for 2010–39, 2040–69, and 2070–99 were presented without indication of relative probability of occurrence. At the time, the suite of projections represented the best assessment of potential future climates. We are now able to compare three climatic periods, 1971–2000, 1981–2010, and 1991–2020 with the trajectory from the 1961–90 climate towards projections for 2010–39.

CLIMATE OF WESTERN ARCTIC CANADA

The climate of Yukon and Mackenzie Valley, including the Mackenzie Delta and western Arctic coast is influenced by its latitude and the St Elias and Coast mountains of the western Cordillera (Fig. 1) (Wahl et al., 1987). The physiography of the region creates a continental climate that supports permafrost (Burn, 1994, 2011). The principal physiographic effects on synoptic climatology stem from the efficacy of the coastal mountains in blocking Pacific maritime air masses from entering the region (Wahl et al., 1987). Thereby, the interior is dryer than the coast with great seasonal range in temperature (Fig. 2). For example, the 98.3 °C range in recorded air temperature

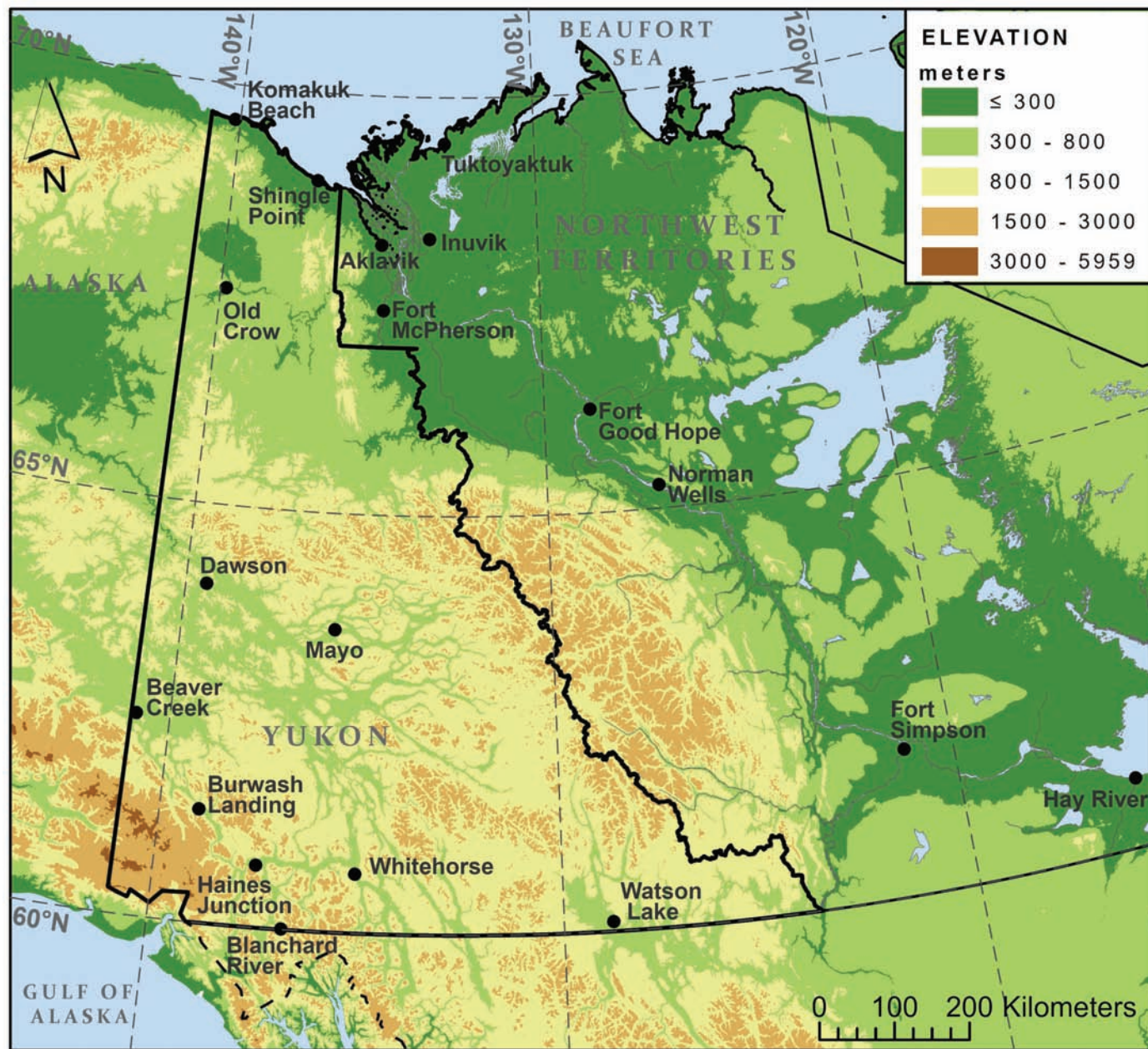


FIG. 1. Yukon Territory and western Northwest Territories, including Mackenzie Mountains and adjacent Mackenzie River valley, with locations of all weather stations used in this paper, except Fort Smith, ESE of Hay River. Elevation data retrieved from ArcticDEM (Porter et al., 2018).

extremes for 1925–2022 at Mayo, YT (Fig. 1), -62.2 to $+36.1$ °C, is the greatest in Canada (Wahl et al., 1987, see also https://climate.weather.gc.ca/historical_data/search_historic_data_e.html). The dissected Cordilleran terrain of much of Yukon facilitates development of steep atmospheric inversions in winter with cold air that pools in valley bottoms, poorly heated due to the low angle of the sun (Fig. 3) (Wahl et al., 1987; Burn, 1993). The climatic gradient in the region is responsible for variation in permafrost distribution from discontinuous permafrost near Whitehorse, YT, and Fort Simpson, NT, through to continuous permafrost near Old Crow, YT, and Inuvik, NT. Mean annual air temperatures (MAAT) for 1981–2010 published by Environment and Climate Change Canada

(ECCC) at https://climate.weather.gc.ca/climate_normals/index_e.html as climate normals for the study area ranged from -0.1 °C at Whitehorse in southern Yukon to -10.1 °C at Tuktoyaktuk, NT, on the western Arctic coast. Mean total annual precipitation in the same period ranged from 553 mm at Blanchard River, YT, to 161 mm at Tuktoyaktuk (Fig. 1).

The low spatial density of climate stations in the region is due to the dispersed population and communities, but the climate records are among the longest in northern Canada. At Fort Simpson the published ECCC record began in 1895; at Dawson in 1897; at Whitehorse continuous records are available since 1940; and they are available for the lower Mackenzie Valley since 1910, the data being principally

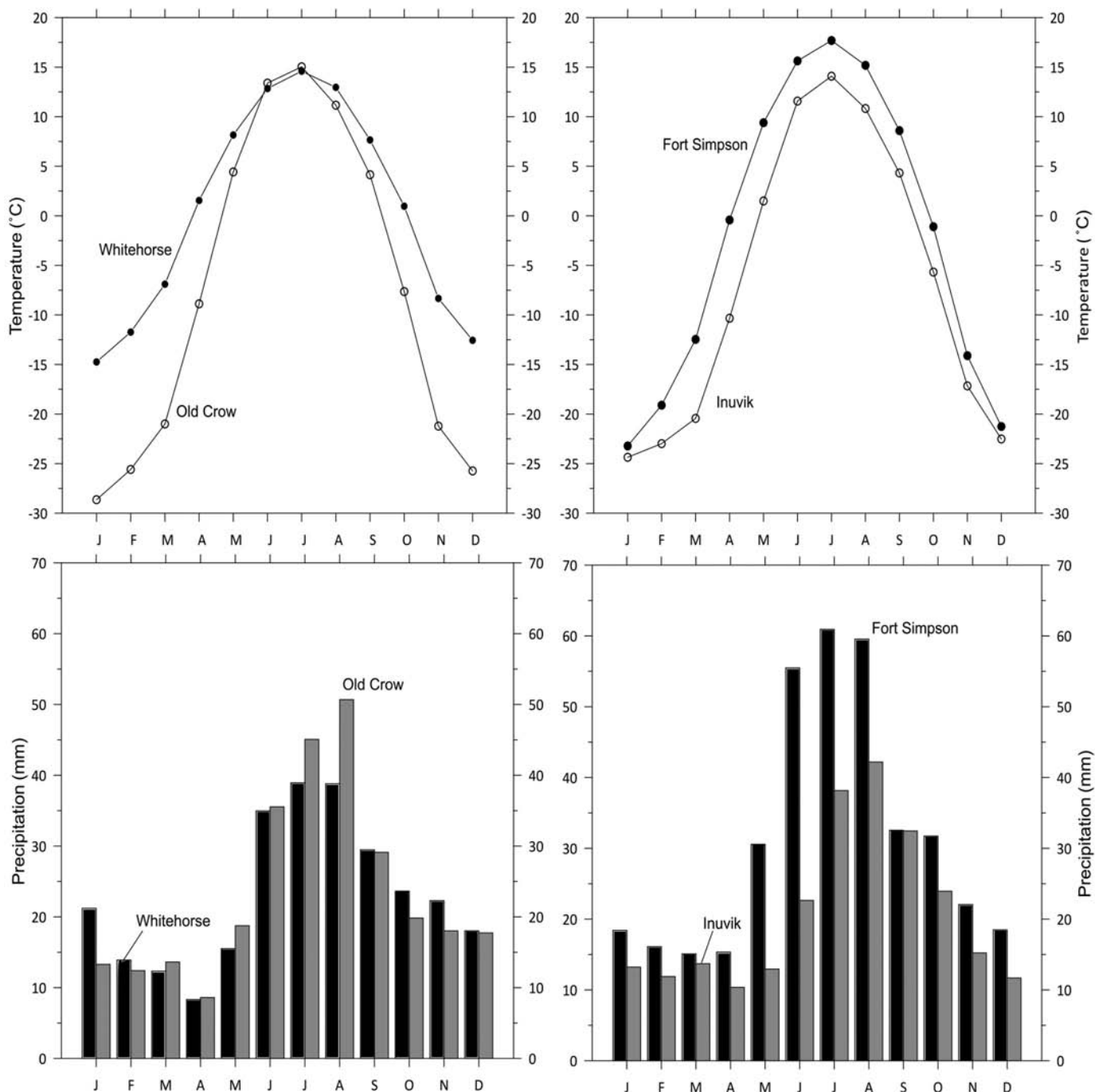


FIG. 2. Monthly mean temperature and precipitation for 1991–2020 at Whitehorse and Old Crow, YT (left-hand panels) and at Fort Simpson and Inuvik, NT (right-hand panels). Whitehorse and Old Crow are 790 km apart, while the distance between Fort Simpson and Inuvik is 920 km. Homogenized ECCO data used for temperature and historical data for precipitation (see text).

from Fort McPherson, Aklavik, Fort Good Hope, and, after 1957, Inuvik. Climate warming during the late 20th century is evident from the record at Dawson and Herschel Island (Fig. 6 in Burn and Zhang, 2009). Thienpont et al., (2013) identified 1970 as the date when the most recent climate warming began in the Mackenzie Delta area. In northwest Canada, MAAT have increased by more than 3 °C at some locations since the mid-20th century, while the rest of Canada experienced an increase of 1.7 °C in this period (Zhang et al., 2019). The rate of increase for annual mean air

temperatures (AMAT) in 1970–2018 has been reported for the Mackenzie Delta area as 0.71 and 0.61 °C decade⁻¹ for Inuvik and Tuktoyaktuk, respectively (Burn et al., 2021a). [MAAT is the mean of several annual means; AMAT is the mean of one year’s data.] Seasonally, rates of temperature increase are greatest in winter (Vincent et al., 2015). These trends are consistent with the reduction of days with snow cover in northern Canada, which have decreased between two and four days decade⁻¹ between 1951 and 2015 (Brown et al., 2017).



FIG. 3. Valley of Lightning Creek, near Keno, central Yukon, in shadow at noon, 23 November 2003. The valley is aligned east – west and is shaded from solar radiation for several months each winter. Photograph © C.R. Burn

TABLE 1. Grid cell size for seven GCMs used to develop climate scenarios for the Mackenzie Gas Project (Table 3 in Burn *et al.* 2004).

GCM	Country	Width (°Latitude)	Width (°Longitude)	Area (km ²)
CCSR98	JPN	5.6	5.6	168,000
CGCM2	CAN	3.75	3.75	74,000
CSIROMk2B	AUS	3.2	5.6	95,000
ESCHAM4	GER	2.8	2.8	41,000
GFDLR30	USA	2.2	3.75	44,000
HADCM3	UK	2.5	3.75	50,000
NCARPCM	USA	2.8	2.8	41,000

CLIMATE SCENARIOS FOR WESTERN ARCTIC CANADA

The Special Report on Emission Scenarios (SRES) (IPCC, 2000) provided several projections of future climate conditions and formed a basis of the Third Assessment Report (IPCC, 2001). These scenarios included ‘storylines’ for future greenhouse gas emissions based on assumptions regarding demographic, social, economic, technological, and environmental driving forces. Forty scenarios were divided into four families (A1, A2, B1, B2). The A1 family assumed

rapid population and economic growth and was further subdivided into three groups based on energy sources: heavy reliance on fossil fuels (A1F1), non-fossil fuel energy sources (A1T), and balanced use of these sources (A1B). The A2 family was regionally focused with respect to development and suggested a continuously increasing population. The B1 and B2 scenarios considered interventions to reduce emissions at the global and local scale, respectively (IPCC, 2000). Global emissions have been within the range of these scenarios and have increased at a rate slightly above the median projection (Fig. 1.28 in IPCC, 2021a).

Since the Fifth Assessment Report (2013), the IPCC has relied on the representative concentration pathway (RCP) scenarios, which define four different emission trajectories, RCP2.6, RCP4.5, RCP6.0, and RCP8.5, based on the magnitude of radiative forcing ($W m^{-2}$) compared to pre-industrial values. The trajectories indicate the heating derived from radiative gases added to the atmosphere, i.e., the enhanced greenhouse effect (Burn *et al.* 2021b). The low-emission RCP2.6 scenario is not comparable to any SRES scenario, but intermediate emission scenario RCP4.5 is comparable to SRES B1 and RCP6.0 lies between SRES B2 and A1B. The high emission scenario RCP8.5 is most similar to the highest SRES scenario A1F1 (van Vuuren

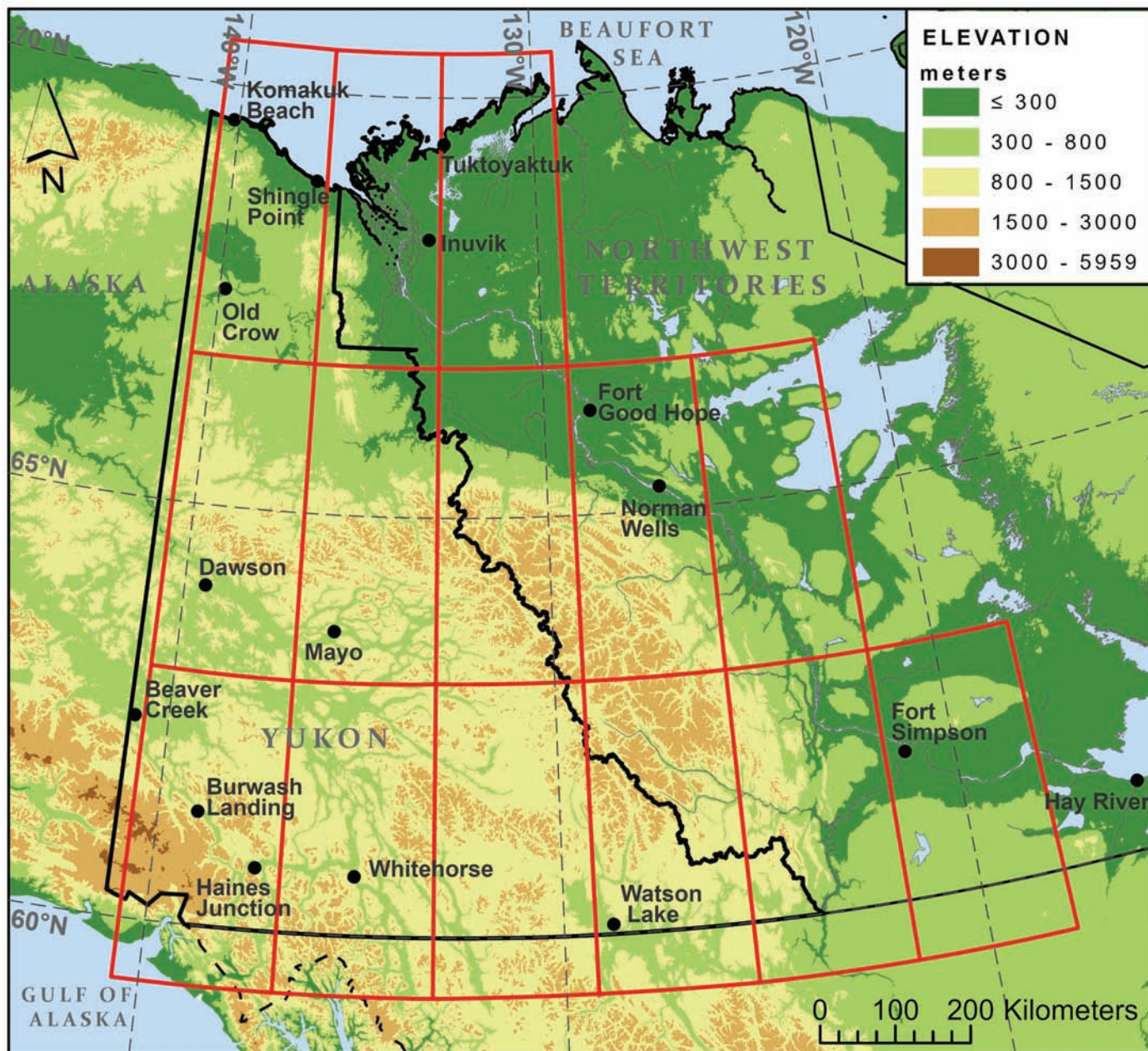


FIG. 4. Grid cells of global climate model CGCM2 from which projections were obtained for comparison with observations of air temperature and precipitation for Yukon and western Northwest Territories. The cell sizes varied between models from which projects were compiled (see Table 1). All stations used to determine regional correlation fields, except Fort Smith, NT, are indicated.

and Carter, 2014). Further emissions-scenario development is reported in the Sixth Assessment (IPCC, 2021a, section 1.6.1.4), but with respect to 2020–50, the range of projected emissions is accommodated by the SRES group, although the specific composition of emissions may vary (Fig. 1.28 in IPCC, 2021a). At global scale, projections of change in temperature have been borne out by observations (Hausfather et al., 2020), demonstrating that the models used by the IPCC are reliable assessments of the global ocean-atmosphere system.

In this paper, we compare the climate scenarios available in 2003, i.e., the SRES group, with the regional climates they projected for northwest Canada. Twenty-nine climate

scenarios from seven global climate models (GCMs) were provided by CCIS (Table 1). In each case, data were extracted for four main regions of interest: central Yukon, southern Yukon, lower (north) Mackenzie Valley, and upper (south) Mackenzie Valley. [Northern Yukon has no stations with records of sufficient length to determine baseline and evolving climate conditions.] Data for each subregion were derived from appropriate grid cells of the various GCMs (Fig. 4). Output data were represented by incremental adjustments from the baseline period of 1961–1990 for three projection periods through the 21st Century (2010–39, 2040–69, and 2070–99). In this analysis, we consider the baseline period and the projections to 2010–39 only.

DATA AND METHODS

The primary data used in this paper are ECCC climate normals for temperature and precipitation. At the time of writing, ECCC had not published data for 1991–2020, the most recent normal period. Normals for temperature were calculated from homogenized historical climate records available up to 2020 at <https://www.canada.ca/en/environment-climate-change/services/climate-change/science-research-data/climate-trends-variability/adjusted-homogenized-canadian-data/surface-air-temperature-access.html>. These data have been homogenized across the country specifically for use in trend analysis and climate change monitoring by correcting for variations in non-climatic factors including changes to instrumentation, local site conditions, observation methodologies, and site relocation (Vincent et al., 2020). The homogenized ECCC records were also used in temperature analyses to determine spatial consistency in climate variation, and to identify representative sub-regional stations with a relatively long record. These are secondary elements of the paper but provide the climatic context for the results of the primary assessment.

Nationally, precipitation data have also been examined and corrected for various factors associated with gauge design, station positioning, and recording interval. Such corrections have made little material difference to the identification of trends in precipitation across Canada, which are spatially inconsistent (Mekis and Vincent, 2011, see <https://www.canada.ca/en/environment-climate-change/services/climate-change/science-research-data/climate-trends-variability/adjusted-homogenized-canadian-data/precipitation.html>). Unlike the homogenized temperature data, homogenized precipitation data are not available through to 2020. As a result, we used historical ECCC data, available to 2020 from https://climate.weather.gc.ca/historical_data/search_historic_data_e.html, to calculate the most recent precipitation normals. [Historical ECCC data were also used to calculate the most recent temperature normal for Beaver Creek, because, unlike all other stations within the study area (Fig. 4), the temperature record has not yet been homogenized for this site.] Published normal values were unavailable in some cases for earlier periods, so historical ECCC precipitation data were used to calculate those missing values.

Climate Records

Several ECCC climate stations with relatively long and complete records were selected for analysis in Mackenzie Valley and Yukon (Fig. 4). For each of the four regions of interest, one station was assigned to be the ‘representative’ station based on length and completeness of record and consistency of data compared to other nearby stations. The representative stations are: Dawson or Mayo (central Yukon), Whitehorse (southern Yukon), Inuvik (lower Mackenzie Valley), and Fort Simpson

(upper Mackenzie Valley). Both Dawson and Mayo are in central, rather than northern, Yukon, but temperature and precipitation records from Old Crow (Fig. 4) have been mainly complete only since 1985 and are insufficient for the analysis. The representative station for central Yukon differed depending on whether temperature (Dawson) or precipitation (Mayo) was considered. Dawson has a longer temperature record, while Mayo has a more complete and consistent precipitation record. The precipitation record for Dawson began in 1901, but has 88 months with missing daily data compared with 23 months at Mayo, where observations began in 1925. At Dawson, the station measuring precipitation has also moved from the townsite to the airport; in Mayo the station has been at the airport throughout the period of record.

ECCC historical meteorological data were tabulated for each location to produce monthly temperature and precipitation records. The tabulated historical temperature and precipitation data were compared with the homogenized series to compare the correlation structures of these series in the region. Data were amalgamated from multiple historical records per location to produce relatively long, complete overall series. The most recent data were commonly from airports with earlier observations at townsites. We considered the different stations at most communities to be close enough that spatial variability in historical temperature and precipitation would be minimal. The airports at Dawson and Fort Simpson are respectively 15 and 12 km from the townsites. Dawson was only used as a representative station for temperature, since spatial variability in air temperature is less than for precipitation (Vincent et al., 2015, 2018).

Guidelines on the calculations of monthly and normal values are provided by ECCC (2020). When determining average temperatures for climate normals, monthly values are excluded if more than three consecutive or five days in total are missing (the “3 and 5 rule”). We followed the “3 and 5 rule” for our tabulations of historical monthly temperatures. For normal total precipitation, monthly values are excluded if any daily data are missing (ECCC, 2020). However, Vincent et al. (2015, 2018) loosened the guideline for precipitation and used the “3 and 5 rule” in their assessments of climate change in Canada. We chose instead to keep months with up to 48 hours or two days of missing precipitation data, a more stringent criterion than used by Vincent et al. (2015, 2018), to improve completeness of the datasets.

In the last 10–15 years many of the stations in the study area have stopped specifically recording rainfall and snowfall, and now only report total precipitation. Of the four representative stations, Mayo and Fort Simpson continue to record precipitation by type. Total precipitation has been reported since October 2007 at Inuvik and November 2012 at Whitehorse. Although we are mainly concerned with total precipitation, monthly rainfall and snowfall were still tabulated for stations that maintain records of these phases. Daily data were also tabulated at these stations to allow

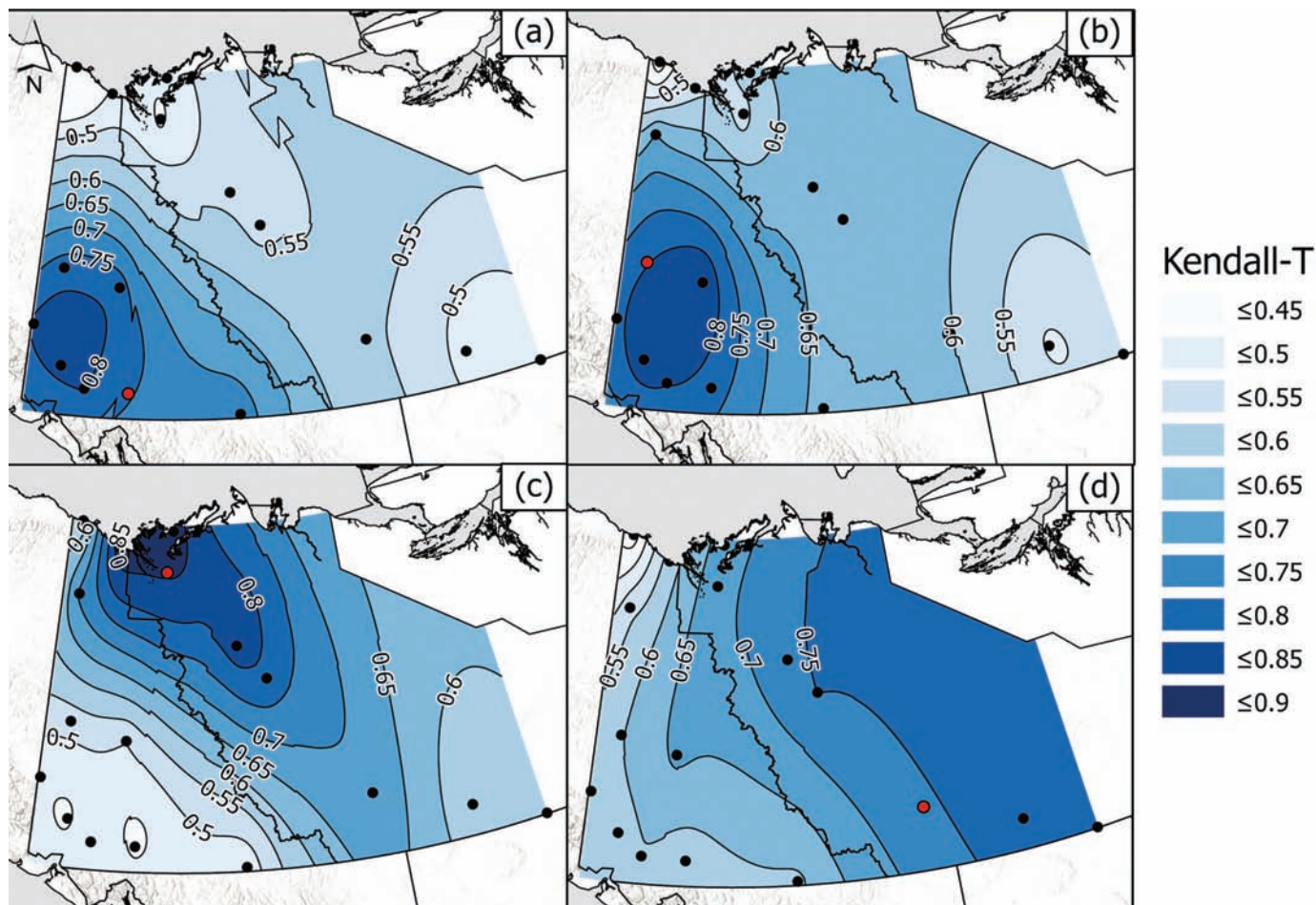


FIG. 5. Spatial correlation fields (Kendall- τ coefficients) for annual mean air temperature relative to the four representative stations of (a) Whitehorse, (b) Dawson, (c) Inuvik, and (d) Fort Simpson. The correlation fields were generated from homogenized climate data.

for assessments of trends in short duration, high intensity summer precipitation events.

Gap Filling

In order to improve the completeness of the *historical* temperature records at the four representative stations and to present a long-term context for climate change, monthly values which did not meet the “3 and 5 rule” were reconstructed using least-squares linear regression with nearby stations, as described by Kokelj et al. (2022:13; see also Henn et al., 2013) (Table A1). Missing daily temperature values at the representative stations were reconstructed based on these relations and combined with available daily temperature values at the representative stations to calculate monthly means. No months required gap filling for Whitehorse. Four months for Dawson were reconstructed with data from Mayo (Jul. 1927, Aug. 1933, Oct. 2008, and Nov. 2008). One month was reconstructed for Inuvik with data from Aklavik (Nov. 1959). Many months prior to 1937 and subsequent months were reconstructed for Fort Simpson with data from Hay River (115 months total). Additionally, a composite temperature record for the lower Mackenzie Valley was produced to extend the record at Inuvik before 1957 to 1910 using

reconstructions with Aklavik (337 months), Fort McPherson (8 months), and Fort Good Hope (218 months).

Regional Correlation

Regional temperature (Fig. 5) and precipitation surfaces were obtained by correlating the homogenized AMAT and historical total annual precipitation (TAP) records for each station with the four representative stations. Following Vincent et al. (2015, 2018), Kendall- τ correlation coefficients were determined since they are derived from a non-parametric method resistant to effects of outliers (Tables 2 and 3) (Reimann et al., 2008). Tables 2 and 3 also present the number of overlapping years of data between each station pair for temperature and precipitation. The spatial correlation surfaces were produced in ArcGIS with ordinary kriging using Kendall- τ coefficients for the station pairs. TAP correlation surfaces are not presented since precipitation is poorly correlated among the stations (Table 3). Kendall- τ correlation coefficients were also computed for adjusted ECCC historical records of temperature and homogenized records of precipitation, for comparative purposes (Tables A2, A3). The difference in correlation coefficients (τ) between the two datasets for temperature was not large

TABLE 2. Kendall- τ correlation coefficients and n for correlation of homogenized annual mean air temperature series from stations in northwest Canada, $p < 0.05$ in all cases. The length of the records at the principal stations, n , are: Whitehorse 76 years, Dawson 112 years, Inuvik 61 years, and Fort Simpson 97 years.

Station	Whitehorse		Dawson		Inuvik		Fort Simpson	
	τ	n	τ	n	τ	n	τ	n
Beaver Creek	0.808	28	0.783	30	0.456	28	0.570	30
Burwash	0.813	43	0.829	43	0.442	43	0.565	43
Dawson	0.772	72	–	–	0.525	59	0.603	89
Fort Good Hope	0.540	47	0.636	46	0.827	36	0.739	47
Fort Simpson	0.553	72	0.603	89	0.689	58	–	–
Fort Smith	0.450	69	0.515	85	0.557	57	0.783	78
Haines Junction	0.802	53	0.803	50	0.493	40	0.607	52
Hay River	0.477	70	0.493	100	0.557	59	0.786	89
Inuvik	0.439	60	0.525	59	–	–	0.689	58
Komakuk Beach	0.288	30	0.362	29	0.562	29	0.319	30
Mayo	0.775	72	0.847	83	0.503	59	0.677	80
Norman Wells	0.532	70	0.631	69	0.787	57	0.760	69
Old Crow	0.517	36	0.653	35	0.706	34	0.560	36
Shingle Point	0.458	29	0.534	28	0.875	30	0.584	28
Tuktoyaktuk	0.470	45	0.590	45	0.878	46	0.676	45
Watson Lake	0.727	72	0.636	76	0.463	57	0.580	75
Whitehorse	–	–	0.772	72	0.439	60	0.553	72

TABLE 3. Kendall- τ correlation coefficients and n for correlation of historical total annual precipitation between stations in northwest Canada. Values in bold indicate $p < 0.05$. The length of the records at the principal stations, n , are: Whitehorse 76 years, Mayo 89 years, Inuvik 61 years, and Fort Simpson 104 years.

Station	Whitehorse		Mayo		Inuvik		Fort Simpson	
	τ	n	τ	n	τ	n	τ	n
Beaver Creek	0.188	32	0.366	30	–0.088	31	0.149	32
Burwash	0.083	41	0.261	41	–0.117	44	0.127	43
Dawson	0.041	69	0.315	80	0.069	53	0.059	90
Fort Good Hope	–0.027	48	–0.043	61	0.170	33	–0.066	72
Fort Simpson	0.119	76	0.104	86	–0.001	61	–	–
Fort Smith	0.096	75	0.199	86	0.045	61	0.167	90
Haines Junction	0.116	42	0.036	41	–0.159	31	0.056	43
Hay River	0.171	74	0.118	86	0.045	59	0.261	96
Inuvik	–0.047	59	0.067	59	–	–	0.001	61
Komakuk Beach	–0.241	29	–0.037	28	0.049	29	–0.030	29
Mayo	0.079	72	–	–	0.067	59	0.104	86
Norman Wells	0.096	75	0.080	72	0.288	60	0.217	76
Old Crow	0.014	30	0.058	28	0.066	27	0.320	30
Shingle Point	–0.243	22	–0.104	22	0.043	22	0.035	22
Tuktoyaktuk	0.180	45	–0.014	45	0.072	41	0.057	46
Watson Lake	0.227	71	0.106	73	0.125	56	0.080	76
Whitehorse	–	–	0.079	72	–0.047	59	0.119	76

with values for the homogenized data being on average 0.02 higher than the historical dataset. For the 60 station pairs, the change in correlation coefficient was > 0.1 at only eight of the pairs (13%) and > 0.05 at 17 of the pairs (28%). Summary data from Student's t -tests for paired values show that the means of correlation coefficients for historical and homogenized data were only significantly different at $\alpha = 0.05$ for the 15 correlations of temperature series with Dawson, where the difference between means was 0.05 (Table A2). For precipitation, the correlation coefficients were on average 0.03 higher for the homogenized dataset. Student's t -tests suggested that the differences between the means of the correlation coefficients for the historical and homogenized datasets were only significantly different at $\alpha = 0.05$ for the 15 Mayo pairs, where the difference between means was 0.04 (Table A3). These comparisons suggest

that there is little fundamental difference between the correlation structures of homogenized and historical ECCO data, but that the homogenization process eliminated some site-specific variation in the data sets.

Climate Trends

Climate trends in 1971–2020 are reported in this paper for several stations (Table 4; Fig. 6). These are the coefficients from least-squares linear regression of the climate variable on time. Time has been plotted on the abscissa (x -axis) and temperature or precipitation on the ordinate (y -axis). Least-squares linear regression is the appropriate method to obtain the coefficients of the relations between the series because time (year) is known with certainty (Mark and Church, 1977).

TABLE 4. Seasonal and annual rates of change in air temperature for 1971–2020 (dT/dt, °C decade⁻¹) for all stations included in the analysis. Homogenized data used for all stations except Beaver Creek.

Months Station	DJF		MAM		JJA		SON		Annual	
	dT/dt	n	dT/dt	n	dT/dt	n	dT/dt	n	dT/dt	n
Dawson	1.15	50	0.39	50	0.22	50	0.22	48	0.48	48
Whitehorse	0.97	48	0.31	48	0.31	48	0.13	48	0.43	48
Inuvik	1.10	50	0.94	50	0.26	50	0.81	48	0.77	48
Fort Simpson	0.92	50	0.27	48	0.22	50	0.40	49	0.44	47
Beaver Creek	0.97	33	0.74	32	0.30	32	0.50	31	0.57	28
Burwash	0.83	46	0.34	49	0.22	48	0.20	45	0.43	41
Fort Good Hope	1.09	36	0.90	34	0.23	34	0.78	34	0.77	29
Fort Smith	0.83	49	0.01	49	0.39	48	0.37	49	0.43	46
Haines Junction	1.17	34	0.26	35	0.18	36	0.06	38	0.38	29
Hay River	0.81	49	0.08	50	0.26	49	0.29	50	0.38	49
Komakuk Beach	0.59	38	0.40	41	0.23	40	0.31	40	0.30	28
Mayo	1.19	48	0.20	48	0.20	49	0.18	48	0.41	47
Norman Wells	1.02	50	0.46	48	0.10	50	0.54	48	0.46	46
Old Crow	1.05	38	0.78	44	0.11	47	0.56	41	0.62	35
Shingle Point	0.78	38	1.01	44	0.24	39	0.64	40	0.62	25
Tuktoyaktuk	0.66	40	0.80	47	0.20	45	0.67	46	0.53	36
Watson Lake	1.03	48	0.27	49	0.20	49	0.19	49	0.43	46

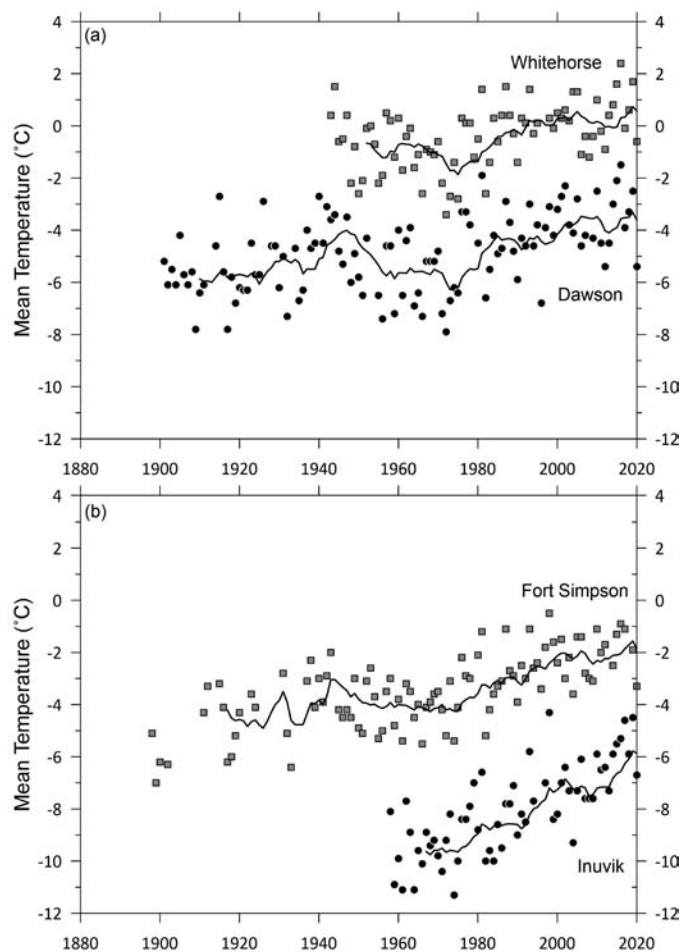


FIG. 6. Annual mean air temperatures for (a) Whitehorse and Dawson, and (b) Fort Simpson and Inuvik. The lines show the running mean of the previous ten years of data. Homogenized data used (see text).

Scenarios

Following Burn et al. (2004), we have ranked the 29 scenarios by projected annual and seasonal changes in both temperature and precipitation and selected high, medium, and low projections (Tables 5 and 6). The projections correspond to the climate scenarios ranked 4th, 15th, and 26th. These rankings are based on the projected changes for the climate variable by the 2010–39 normal period relative to the baseline period of 1961–90. The three highest and lowest projections were not used in order to obtain a conservative estimate of the extremes and to exclude far outliers.

CLIMATE CHANGE IN WESTERN ARCTIC CANADA

Temperature – Spatial Coherence

Maps displaying correlation fields for AMAT in the study region are presented in Fig. 5. Correlation fields are presented with respect to Whitehorse, Dawson, Inuvik, and Fort Simpson. Correlation of temperature series with themselves were omitted during kriging to avoid presenting an artificially peaked distribution centered on the station. The correlation coefficients are relatively high for stations near the representative locations, indicating the subregional coherence of climate variation throughout the extant record. Correlation of AMAT is consistently high along Mackenzie Valley and within south and central Yukon. Data from northern Yukon are most closely correlated with stations in the Mackenzie Delta area.

Temperature – Temporal Records

Air temperatures have been increasing nationally since 1970 with particularly high rates of warming in Canada’s

TABLE 5. Climate change scenarios for 2010–39 relative to the baseline (1961–90) for four regions in NW Canada ranked by increase in mean seasonal or annual temperature (°C) (Burn et al. 2004). Climate normals for homogenized data (Vincent et al. 2020) are provided for the baseline with observed relative changes for the three following intervals.

Months	DJF	MAM	JJA	SON	Annual
Southern Yukon (Whitehorse)					
Ranked projected increase in seasonal or annual temperature					
4th	2.5	1.7	1.9	2.2	1.8
15th	1.0	1.0	1.2	1.4	1.1
26th	0.4	0.6	0.5	0.7	0.9
Observed baseline temperature					
1961–1990	-15.6	-0.1	12.6	-0.5	-0.9
Observed change relative to baseline					
1971–2000	+0.7	+0.6	+0.2	+0.2	+0.4
1981–2010	+2.3	+0.8	+0.5	+0.2	+1.0
1991–2020	+2.5	+1.0	+0.9	+0.6	+1.2
Central Yukon (Dawson)					
Ranked projected increase in seasonal or annual temperature					
4th	3.0	1.8	2.7	2.9	2.2
15th	1.6	1.2	1.1	1.9	1.4
26th	0.9	0.7	0.5	1.1	1.1
Observed baseline temperature					
1961–1990	-26.1	-2.6	13.4	-5.5	-5.2
Observed change relative to baseline					
1971–2000	+0.6	+1.0	+0.5	-0.3	+0.5
1981–2010	+2.3	+1.3	+0.6	+0.0	+1.1
1991–2020	+2.8	+1.5	+0.9	+0.3	+1.4
Lower Mackenzie Valley (Inuvik)					
Ranked projected increase in seasonal or annual temperature					
4th	3.1	2.2	2.2	3.3	2.4
15th	2.0	1.6	1.1	2.1	1.6
26th	1.1	0.9	0.4	1.1	1.3
Observed baseline temperature					
1961–1990	-26.5	-12.4	11.2	-8.5	-9.0
Observed change relative to baseline					
1971–2000	+1.1	+1.1	+0.5	+0.4	+0.7
1981–2010	+2.1	+1.7	+0.7	+0.9	+1.3
1991–2020	+3.2	+2.6	+1.0	+2.3	+2.3
Upper Mackenzie Valley (Fort Simpson)					
Ranked projected increase in seasonal or annual temperature					
4th	2.5	2.4	1.9	2.7	2.1
15th	1.5	1.4	1.1	1.5	1.3
26th	0.6	0.6	0.6	0.9	1.0
Observed baseline temperature					
1961–1990	-23.8	-2.5	15.4	-3.5	-3.6
Observed change relative to baseline					
1971–2000	+0.9	+1.0	+0.3	+0.3	+0.7
1981–2010	+1.9	+1.1	+0.5	+0.7	+1.1
1991–2020	+2.5	+1.3	+0.8	+1.3	+1.5

western Arctic (Zhang et al., 2019). Warming in the region has been concentrated in winter (Vincent et al., 2015; Bush and Lemmen, 2019). Both of these phenomena are consequences of Polar Amplification of climate change, due to reduction in ice cover and albedo, increased transport of latent heat to polar latitudes, and reduced net

loss of long-wave radiation with near-surface warming (IPCC, 2021a, Section 7.4.4.1.1). In Yukon and Mackenzie Valley (Fig. 6, Table 4), the greatest increase in AMAT in 1971–2020, using homogenized values, has been at Inuvik at a rate of 0.77°C decade⁻¹. At Dawson, Whitehorse, and Fort Simpson, AMAT has increased between 0.43 and 0.48°C decade⁻¹. The lowest rate of increase in AMAT, 0.30°C decade⁻¹, was recorded over the relatively short record of 28 complete years at Komakuk Beach, YT, in 1971–2015. Seasonal warming in winter has been between 0.59 and 1.19°C decade⁻¹ at Komakuk Beach and Mayo, respectively (Table 4).

Increases in 10-year average temperatures more readily demonstrate the magnitude of climate change than the 30-year climate normals in cases where change has been unidirectional and continuous. For Inuvik, the difference in MAAT between 1961–70 and 2011–20 has been 3.7°C, and at Whitehorse 1.7°C. At Dawson and Fort Simpson, the increases in MAAT over the same period have been similar to data from Whitehorse, namely 2.0°C at Dawson and 2.3°C at Fort Simpson. The MAAT, calculated over 10 years, is now -5.9°C at Inuvik, -3.6°C at Dawson, -1.8°C at Fort Simpson, and 0.6°C at Whitehorse.

Temperature – Projections

The warming recorded at each of the four representative stations indicates the 30-year MAAT may meet or exceed the upper CCIS projections for annual and winter air temperatures in 2010–39 (Table 5, Fig. 7). MAAT in 1991–2020 increased by between 1.2°C at Whitehorse and 2.3°C at Inuvik relative to 1961–90 (Fig. 7). Mean winter temperatures have already exceeded the upper projections for 2010–39 at Inuvik and are approaching the upper projections for the other three locations, 20 years in advance of this period (Fig. 7). Winter conditions in lower Mackenzie Valley are now warmer than they were in upper Mackenzie Valley 30 years ago. For spring, summer, and autumn, current temperature trends are progressing towards the mid- to upper-level projections. Mean spring temperatures have already exceeded the change projected for 2010–39 in the lower Mackenzie Valley (Table 5).

Precipitation – Spatial Coherence

Precipitation records are poorly correlated between stations with Kendall- τ coefficients generally ranging from 0.1 to 0.3 (Table 3). The majority of correlations between stations are not statistically significant. Long-term precipitation records are available for Whitehorse, Mayo, Inuvik, and Fort Simpson (Fig. 8). Figure 8 displays considerable variation between stations in precipitation trends, even though the climate scenarios generally anticipated greater precipitation within the region over time (Table 6).

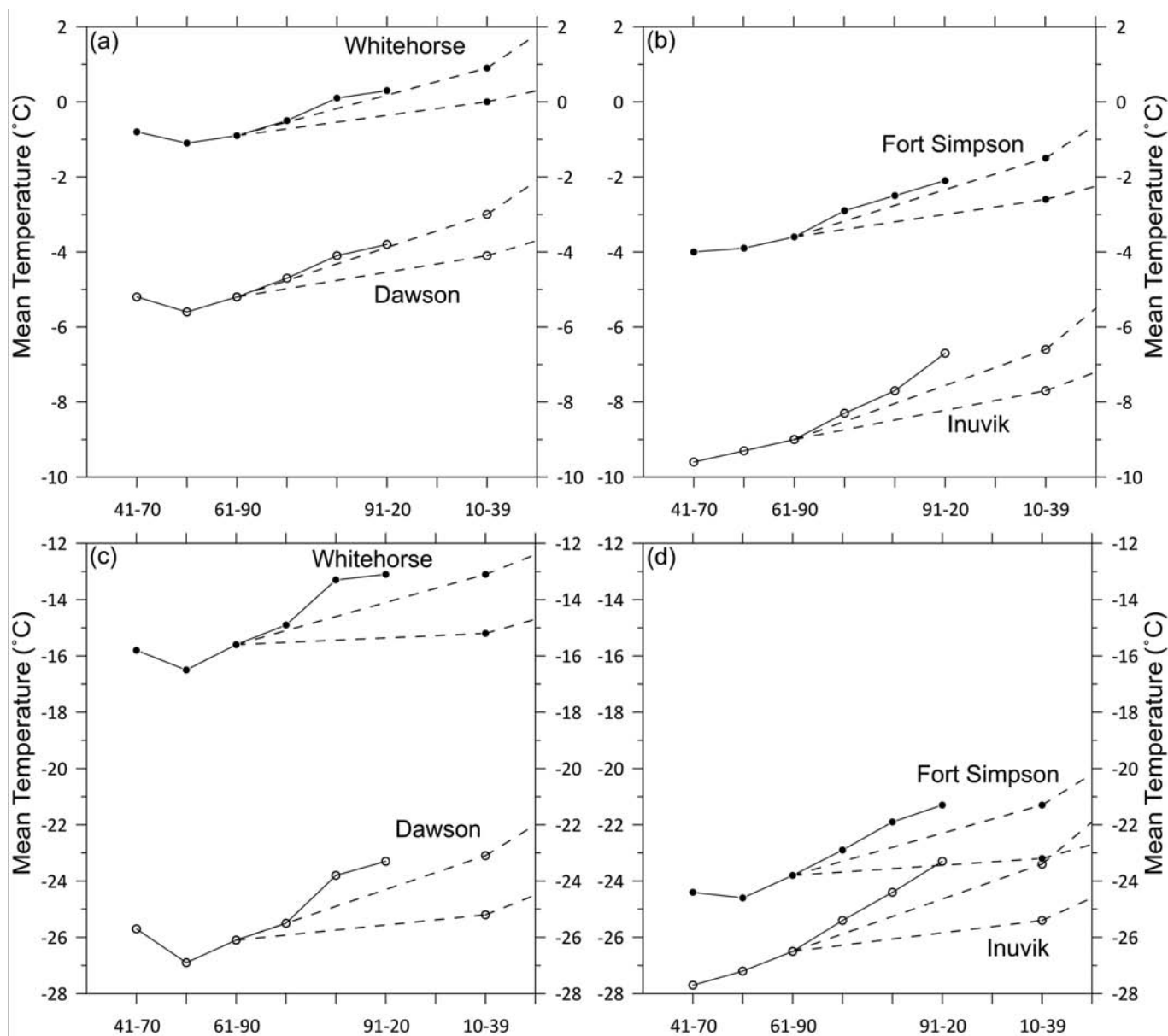


FIG. 7. Comparison of observed and projected (a, b) mean annual and (c, d) mean winter air temperatures for the four representative stations. Solid lines show the observed air temperature as climate normals for 1941–70 to 1991–2020 computed from homogenized series (see text). Dashed lines show projections from the 1961–90 baseline.

Precipitation – Temporal Trends

Hartmann et al. (2013) and Bintanja and Andry (2017) suggest that certain aspects of the precipitation regime may be expected to change with temperature. The frequency distributions of total annual rainfall (TAR), TAP, and August and September rainfall are presented in Figure 9 for Mayo and Norman Wells as normal probability plots. Precipitation magnitude has been plotted against probability of exceedance. Data are presented for 1961–2020, i.e., 60 years of observations. If events were distributed evenly through the 60 years, each 20-year interval would contribute six or seven events to the upper, middle, and lower thirds of the distributions. In fact, recent TAR values (2001–20) are overrepresented in the upper

end of the distribution (Figs 9a, 9b). At both Mayo and Norman Wells, 9 of the 20 years in 2001–20 are in the upper third of the distributions. Similar results are observed in the frequency distribution of TAP for Mayo and Norman Wells (Figs 9c, 9d) where 8 and 9 of the respective wettest years occurred during 2001–20. Warming of the shoulder seasons (i.e., early autumn and spring) has resulted in a change in form of precipitation, with snowfall being replaced by rainfall (Vincent et al., 2015). With respect to August and September rainfall, Figs 9e and 9f show that the most recent years are overrepresented in the upper third of the frequency distributions with 11 and 12 years from 2001–20 for Mayo and Norman Wells respectively. Similar analyses for Fort Simpson and Hay River also suggest increases in precipitation, especially for TAR and

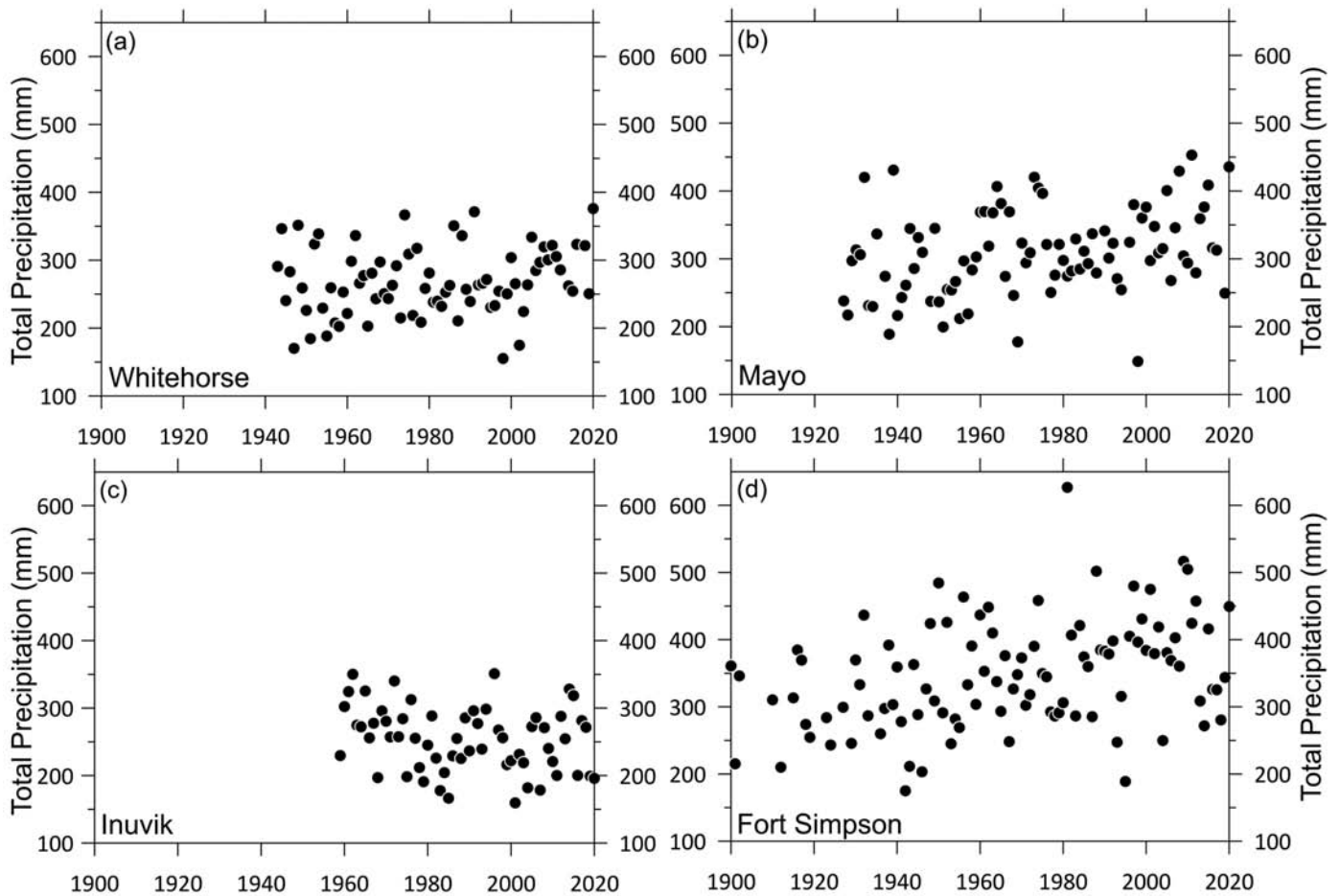


FIG. 8. Annual total precipitation for (a) Whitehorse, (b) Mayo, (c) Inuvik, and (d) Fort Simpson over the period of record. ECCC historical data used. No extension or gap filling of records has been undertaken due to the spatial variability of this index.

August and September rainfall. The proportion of total precipitation falling as rain has increased recently at Mayo where 10 years of 2001–20 are represented in the upper third of the distribution (Fig. 10). The proportion is not as great at the other three stations where rainfall is specifically recorded.

For infrastructure, changes in short-term, high-intensity precipitation events may be of greater concern than overall changes on an annual basis (Zhang et al., 2019, p. 168). However, maximum 1, 2, and 3-day summer (June–September) precipitation totals do not appear more frequently than the expected 6 or 7 times in the upper 20 years of the distributions.

Precipitation – Projections

The observed seasonal and projected annual total precipitation relative to the 1961–90 baseline is presented in Figure 11 and Table 6. No consistent behaviour with respect to the projections can be identified for mean (normal) TAP. The values recorded at Inuvik have been lower than projected while data for Mayo, Whitehorse, and Fort Simpson are consistent with middle projections in 1991–2020. Relative to the 1961–90 climate, total

annual precipitation for 1991–2020 increased by 2.6% at Mayo 3.2% at Whitehorse, and 4.4% at Fort Simpson and decreased by 3.3% at Inuvik. On an annual or seasonal basis, no common trend over time can be determined in total precipitation for these four stations (Fig. 11; Table 6).

DISCUSSION

The purpose of this paper is to determine, relatively, which scenarios for climate change available in the early 2000s have best projected the subsequent record. With respect to precipitation there has been little overall correspondence between projections and observations. Variations in precipitation over time within the region are neither spatially nor temporally consistent. No clear trends in TAP have been observed in 1991–2020 (Figs 8, 11), even though all scenarios indicated precipitation would be higher in 2010–39 than during the 1961–90 baseline period (Table 6). There is, however, some evidence that the nature of precipitation is changing, with greater proportion of the total now falling as rain (Fig. 10). This has been anticipated in other articles (e.g., Bintanja and Andry, 2017). The trend is not (yet) statistically significant, due to the variability in

TABLE 6. Climate change scenarios for 2010–39 ranked by change from the baseline (1961–90) in total seasonal or annual precipitation (%) for all four regions (Burn et al. 2004). Climate normal data (mm) are provided for the baseline with observed relative changes for the three following intervals. Normal values in italics were calculated from ECCC historical climate data while other values were obtained directly from ECCC.

Months	DJF	MAM	JJA	SON	Annual
Southern Yukon (Whitehorse)					
Ranked projected change in seasonal or annual precipitation (%)					
4th	+12.3	+13.8	+8.9	+12.2	+9.6
15th	+5.6	+6.5	+4.2	+6.6	+7.4
26th	+0.4	+1.9	-2.3	+3.7	+2.1
Observed baseline precipitation (mm)					
1961–1990	47.7	34.8	109.0	77.1	268.8
Observed change relative to baseline (%)					
1971–2000	-2.3	-6.3	1.9	0.0	-0.5
1981–2010	-3.8	-3.4	-2.5	-0.6	-2.4
1991–2020	9.9	2.6	3.4	-2.3	3.2
Central Yukon (Mayo)					
Ranked projected change in seasonal or annual precipitation (%)					
4th	+13.7	+13.1	+10.4	+16.3	+10.4
15th	+8.0	+7.7	+4.1	+8.6	+6.8
26th	+0.4	+1.4	-2.1	+1.5	+1.7
Observed baseline precipitation (mm)					
1961–1990	55.8	39.4	137.2	85.9	318.4
Observed change relative to baseline (%)					
1971–2000	-13.6	8.4	-0.4	-0.7	-1.7
1981–2010	-8.4	6.3	-2.5	1.0	-1.5
1991–2020	-7.3	4.1	7.5	2.4	2.6
Lower Mackenzie Valley (Inuvik)					
Ranked projected change in seasonal or annual precipitation (%)					
4th	+15.4	+17.9	+14.6	+14.6	+11.8
15th	+6.0	+5.6	+6.1	+9.3	+7.4
26th	+0.8	+0.2	-0.1	2.0	+2.1
Observed baseline precipitation (mm)					
1961–1990	43.5	42.5	100.2	71.3	257.4
Observed change relative to baseline (%)					
1971–2000	-5.5	-9.4	-5.0	3.5	-3.5
1981–2010	-7.1	-8.2	-8.5	-2.2	-6.5
1991–2020	-17.4	-12.9	3.9	0.4	-3.3
Upper Mackenzie Valley (Fort Simpson)					
Ranked projected change in seasonal or annual precipitation (%)					
4th	+17.6	+22.5	+9.7	+12.6	+9.6
15th	+7.8	+8.2	+2.7	+6.0	+6.2
26th	-1.0	-1.6	-1.4	+2.3	+0.9
Observed baseline precipitation (mm)					
1961–1990	56.3	63.8	148.3	92.0	360.5
Observed change relative to baseline (%)					
1971–2000	-3.0	-5.8	10.7	-2.0	2.4
1981–2010	-1.2	-3.1	17.2	4.8	7.5
1991–2020	-5.3	-4.4	18.6	-6.2	4.4

observations throughout the records. It is visually apparent that data since 2000 are overrepresented in the higher tails of the rainfall distributions examined here (Fig. 9).

In contrast, annual and seasonal mean air temperatures are spatially coherent within the region, and all have

increased since 1971 (Figs 5, 6). The rates of annual increase are generally highest in the lower Mackenzie valley and northern Yukon. The rates of warming exceed or approach the higher projections of the increase between the baseline and 2010–39 (Figs 6, 7). The highest projections published in 2000 were from scenarios that mimic the high emissions pathway for RCP8.5. During 1991–2020, therefore, regional temperature has followed the projections of high emission scenarios. The rate of increase in AMAT has varied spatially within the region from 0.30 to 0.77 °C decade⁻¹ since 1971. If scenarios of future climate change are to be chosen on the basis of past performance, the projections for highest climate change should be seriously considered.

The changes in temperature that have been compared with climate projections are 30-year averages. The continuous warming appears greater when examined at 10-year resolution due to its continuity. The IPCC’s Sixth Assessment projects that under any climate scenario, the warming will continue globally for at least two more decades and for longer if reductions are not made in anthropogenic greenhouse gas emissions (Fig. SPM.8 in IPCC, 2021b). The Sixth Assessment also states that “it is *virtually certain* that the Arctic will continue to warm more than global surface temperature, with *high confidence* above two times the rate of global warming” (IPCC, 2021b, SPM B.2.1, italics in original; see also Rantanen et al., 2022). The regional distribution of this projected warming includes much of the study area of this paper (Fig. SPM.5 in IPCC, 2021b). The historical record, its correspondence with higher projections for temperature change in 1991–2020, and the IPCC’s confidence that climate change will be more rapid at high latitudes, all suggest that it is prudent to consider relatively high model projections for climate change in the study area over the next 20–30 years. If present rates of change are sustained (1971–2020; Table 4), then current values for climate normal MAAT (1991–2020; Table 5) of +0.3, -2.1, -3.8, and -6.7°C at Whitehorse, Fort Simpson, Dawson, and Inuvik, respectively, may rise to +2.5, +0.1, -1.4, and -2.8°C by 2041–70. Taken on a decadal basis, current values for MAAT (2011–20) of +0.6, -1.8, -3.6, and -5.9°C may rise to +2.8, +0.4, -1.2, and -2.0°C at the respective locations by 2061–70, i.e., in 50 years’ time. Fifty years is a normal service life for infrastructure.

Air temperature is one of the variables that controls the state of permafrost, which responds to changes in surface conditions including climate (e.g., Burn and Kokelj, 2009). Mean annual ground temperatures are commonly higher than MAAT principally due to the effects of snow (e.g., Smith and Riseborough, 2002). Changes in surface conditions, including atmospheric warming, have induced increases in near-surface permafrost temperatures within the Canadian western Arctic and circumpolar world (e.g., Burn and Kokelj, 2009; Smith et al., 2012, 2022). Warming of near-surface permafrost characteristically lags increases in air temperature due to latent heat sinks associated with

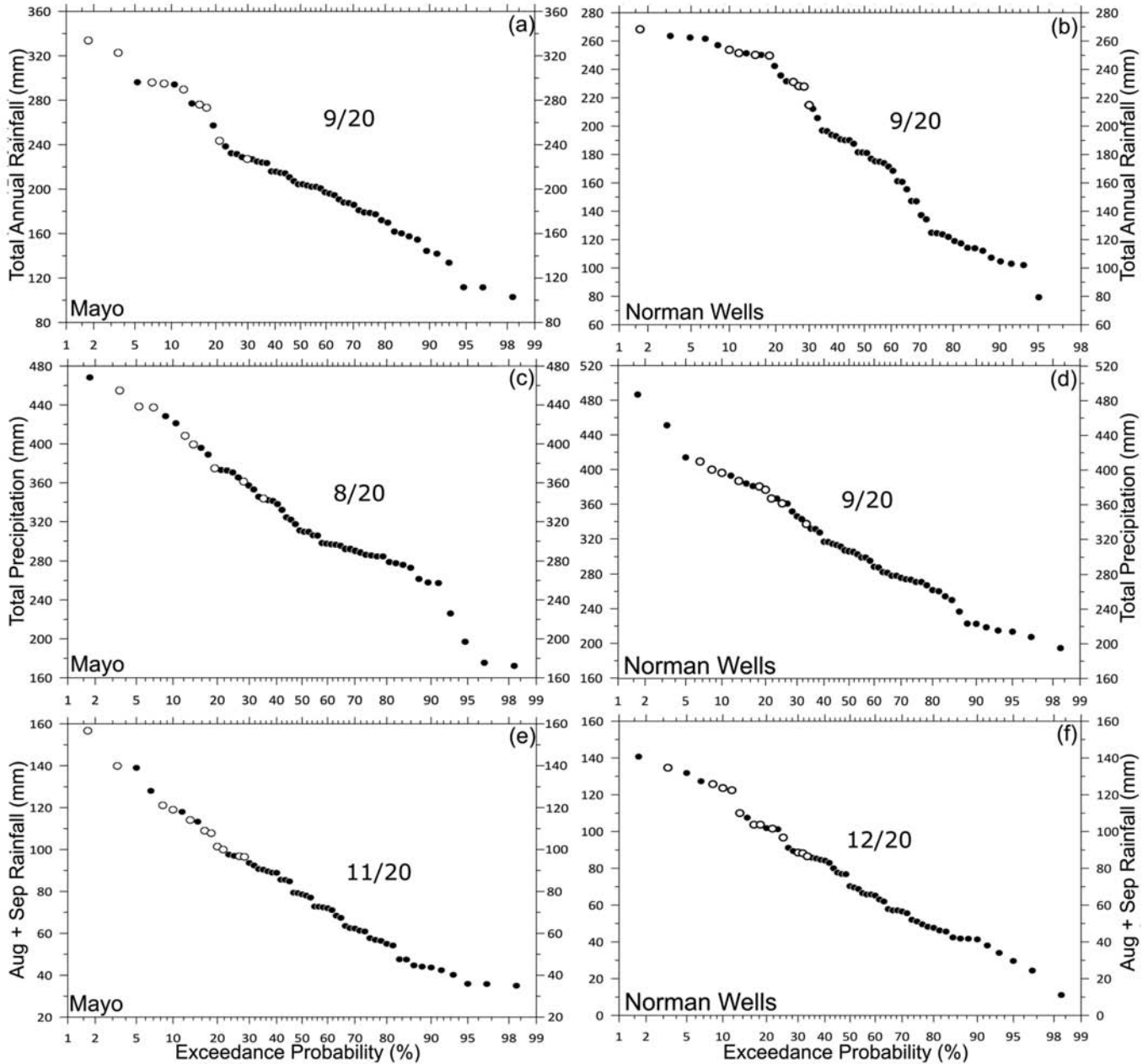


FIG. 9. Exceedance probability distributions for (a) TAR, (c) TAP, (e) August and September rainfall at Mayo, YT, and (b) TAR, (d) TAP, and (f) August and September rainfall at Norman Wells, NT, 1961–2020. Open circles are years from 2001–20 in the upper third of the distribution (also listed as a fraction of the 20 upper years). The exceedance probability is normally distributed.

melting pore and excess ground ice (Smith et al., 2022), and propagation of heat into colder permafrost at depth (e.g., Burn and Zhang, 2009, 2010). Nevertheless, given the record of regional climate warming exceeding the upper-level scenarios, the millennial time scales required to reverse recent changes to atmospheric greenhouse-gas concentrations (Burn et al., 2021b), and MAAT already $> 0^{\circ}\text{C}$, near-surface permafrost will likely become unsustainable, i.e., it will begin, or continue, to thaw at locations in central and southern Yukon and adjacent Mackenzie Valley over the next two decades. It may still take centuries for permafrost to thaw at depth (e.g., Burn, 1998).

Warming of permafrost has two principal geotechnical consequences for engineering design: reduction in strength of adfreeze bonds for pile foundations and acceleration of creep deformation under an applied load (Hjort et al., 2022). In addition, thawing of ice-rich permafrost leads to substantial loss of bearing strength. The thermal regimes of infrastructure foundations are affected by the structures themselves and by lateral heat exchange with the surrounding ground. As a result, infrastructure stability is not isolated from the effects of climate change on the permafrost thermal regime. Zhou et al. (2008) demonstrated the sensitivity of foundation integrity to various scenarios for climate warming using geothermal

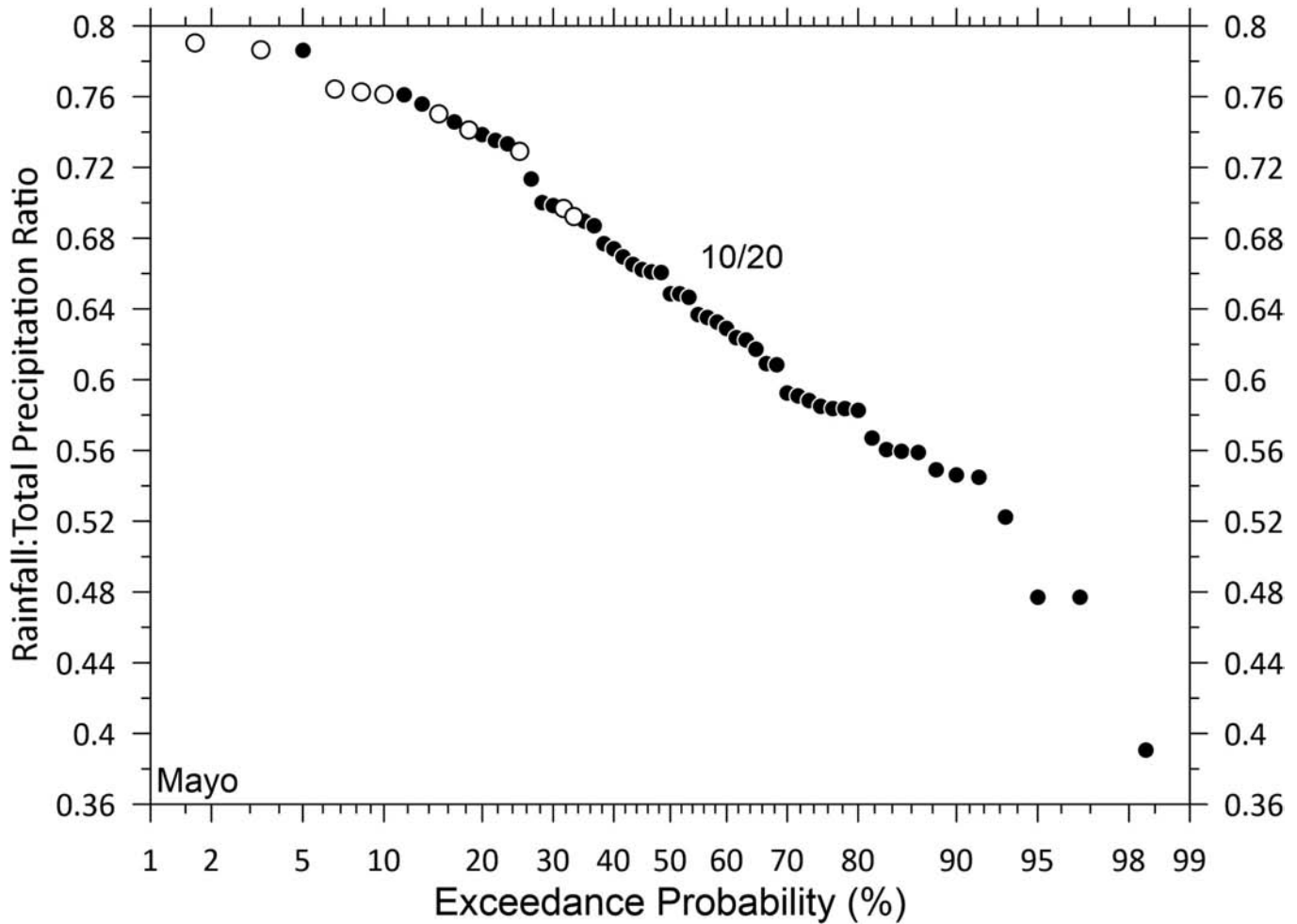


FIG. 10. Exceedance probability distribution for ratio of TAR to TAP in 1961–2020 at Mayo, YT. Open circles are years from 2001–20 in the upper third of the distribution (also listed as a fraction of the 20 upper years). The exceedance probability is normally distributed.

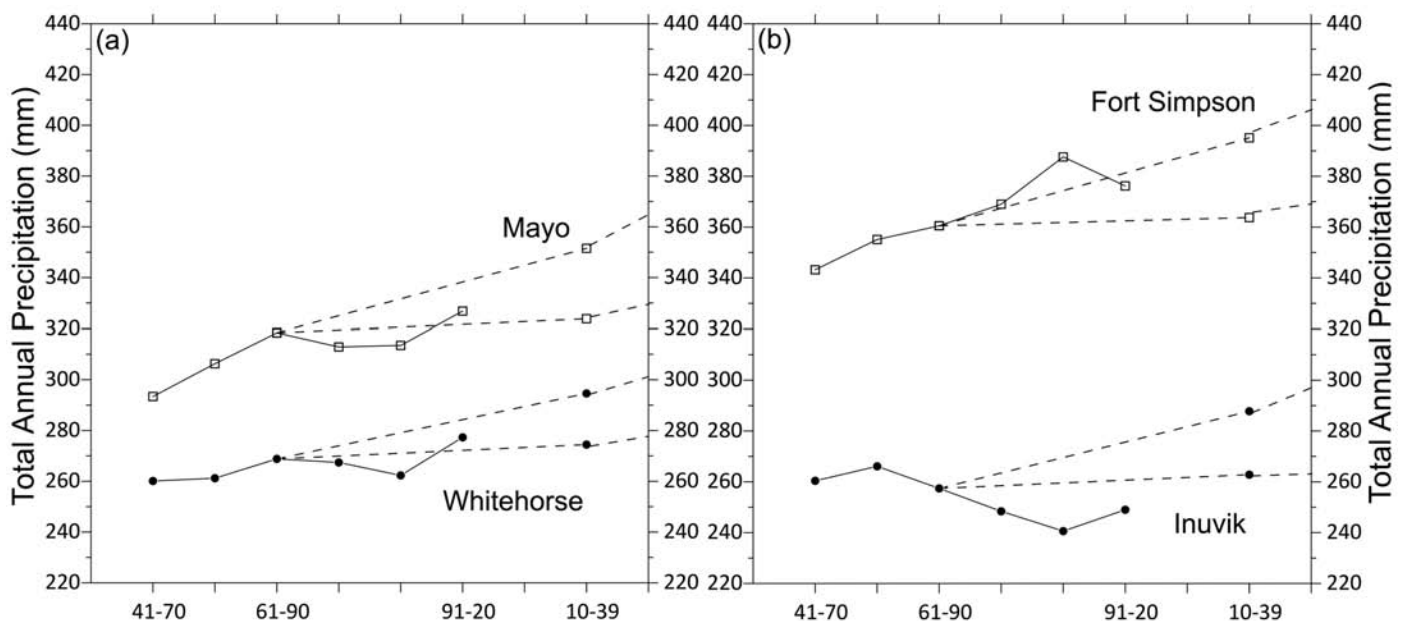


FIG. 11. Comparison of observed and projected total annual precipitation for (a) Mayo and Whitehorse, and (b) Fort Simpson and Inuvik. Solid lines show the observed precipitation from climate normals in 1941–70 to 1991–2020. Data for 1941–71 to 1981–2010 from Canadian Climate Normals (ECCC 2020); 1991–2020 means computed from historical data (see text). Dashed lines show projections from the 1961–90 baseline.



FIG. 12. Thermosyphons installed along the Alaska Highway at Dry Creek, YT (km 1840). These passive ground cooling installations are required to prevent a body of massive ice beneath the road from thawing. Photograph taken on 31 July 2021, © C.R. Burn.

simulation for buildings at Inuvik. Under an upper-level climate scenario, as has occurred to date, the foundations of a majority (74%) of the buildings in the town are projected to be adversely affected by 2069 (Table 1 in Zhou et al., 2008). The proportion of affected buildings is expected to vary with near-surface ground conditions within the town site.

The prospect of relatively high rates of climate warming continuing in Yukon and Mackenzie Valley has two principal implications for foundation design in permafrost. First, it suggests that increased investment in site investigation to identify thaw-stable sites may be a prudent planning strategy for infrastructure projects, especially for municipal and transportation infrastructure that occupy a large footprint (e.g., see National Standard of Canada CAN/BNQ 2501-500/2017). In the southern portions of the permafrost regions such a strategy may mean facilities might not be located with great convenience, but their service life would be extended. Second, rising winter temperatures imply that the operational efficacy of thermosyphons, used to chill foundations, may be impeded. As a result, at sites where preservation of frozen ground is essential for infrastructure integrity, the number of required thermosyphons may increase and detailed design configurations will be required (Hayley and Horne, 2008; Canadian Standards Association, 2019). This will almost certainly lead to cost increases, as at the Dry Creek site at km 1840 on the Alaska Highway in southwest Yukon where installation of 58 thermosyphons to prevent thawing of massive ice below less than half a kilometre of the highway in 2020 cost CAD \$4 million (Fig. 12) (Loranger et al., 2015; Muhammad Idrees, Yukon Highways and Public Works, pers. comm., 2021). Such costs prohibit installation of thermosyphons beneath numerous kilometres of highway

embankment and raise the cost effectiveness of thorough site investigations and alternative route selections.

CONCLUSIONS

The following conclusions may be drawn from this paper:

- There is sub regional consistency in temperature variation, such that Yukon and adjacent Northwest Territories may be considered in two principal climatic subregions: south and central Yukon, and Mackenzie River valley.
- Within the region, the rate of increase in recorded annual mean temperatures has ranged from 0.30 to 0.77 °C decade⁻¹ since 1971; the magnitude of the warming has been up to 2.3 °C in 30-year mean temperatures and 3.7 °C in 10-year means.
- The observed changes in MAAT have exceeded the track to the higher projections of climate warming for 2010–39 made in 2000.
- Warming in winter has exceeded the track to the higher projections for 2010–39 made in 2000.
- There has been little consistency in regional total precipitation series, but at two of four sites where rainfall is specifically recorded, more annual rainfall totals from 2001–20 than would be expected in a stationary series were observed in upper portions of the 60-year record.
- Due to the high rate of climate change, developers may consider enhancing site investigations for projects in southern parts of the region to select locations with thaw stable soils for construction.

ACKNOWLEDGEMENTS

This paper was stimulated through conversations with D.W. Hayley, who co-led the Canadian Standards Association's development of CSA PLUS 4011:19 in 2009–10 and its revision in 2018–19. The research is part of a long-term program assessing climate change and its effects on the permafrost environment in Yukon and the western Arctic supported by the Natural Sciences and Engineering Research Council of Canada; the Polar Continental Shelf Project, Natural Resources Canada;

the Northern Transportation Adaptation Initiative, Transport Canada; Yukon Highways and Public Works; the First Nation of Na-Cho Nyak Dun; the Aurora Research Institute; and the Northern Science Training Program, Crown-Indigenous Relations and Northern Affairs Canada. We thank Lucie Vincent and Ian McKendry for help during preparation of this paper, and three anonymous referees for their kind, generous, and helpful comments. Their suggestions are appreciated by adoption. Astrid Schetselaar is supported by the NSERC PermafrostNet Strategic Network (funding reference number NETGP 523328 – 18).

REFERENCES

- Bintanja, R., and Andry, O. 2017. Towards a rain-dominated Arctic. *Nature Climate Change* 7(4):263–267.
<https://doi.org/10.1038/nclimate3240>
- Bonsal, B.R., and Kochtubajda, B. 2009. An assessment of present and future climate in the Mackenzie Delta and the near-shore Beaufort Sea region of Canada. *International Journal of Climatology* 29(12):1780–1795.
<https://doi.org/10.1002/joc.1812>
- Brown, R., Schuler, D.V., Bulygina, O., Derksen, C., Luojus, K., Mudryk, L., Wang, L., and Yang, D. 2017. Arctic terrestrial snow cover. In: Symon C., ed. *Snow, water, ice and permafrost in the Arctic (SWIPA) 2017*. Oslo: Arctic Monitoring and Assessment Programme. 25–64.
<https://www.amap.no/documents/doc/snow-water-ice-and-permafrost-in-the-arctic-swipa-2017/1610>
- Burn, C.R. 1993. Comments on “Detection of climatic change in the western North American Arctic using a synoptic climatological approach” by Laurence S. Kalkstein, Paul C. Dunne, and Russel S. Vose. *Journal of Climate* 6(7):1473–1475.
[https://doi.org/10.1175/1520-0442\(1993\)006<1473:COOCCI>2.0.CO;2](https://doi.org/10.1175/1520-0442(1993)006<1473:COOCCI>2.0.CO;2)
- . 1994. Permafrost, tectonics, and past and future regional climate change, Yukon and adjacent Northwest Territories. *Canadian Journal of Earth Sciences* 31(1):182–191.
<https://doi.org/10.1139/e94-015>
- . 1998. The response (1958–1997) of permafrost and near-surface ground temperatures to forest fire, Takhini River valley, southern Yukon Territory. *Canadian Journal of Earth Sciences* 35(2):184–199.
<https://doi.org/10.1139/e97-105>
- . 2003. Climate change scenarios for the Mackenzie Gas Project. Northern Water Resource Studies, Water Resources Division, DIAND, Yellowknife.
- . 2011. Permafrost distribution and stability. In: French, H. and Slaymaker, O. eds. *Changing cold environments - a Canadian perspective*. New York: John Wiley & Sons Ltd. 126–146.
<https://doi.org/10.1002/9781119950172.ch7>
- Burn, C.R., and Kokelj, S.V. 2009. The environment and permafrost of the Mackenzie Delta area. *Permafrost and Periglacial Processes* 20(2):83–105.
<https://doi.org/10.1002/ppp.655>
- Burn, C.R., and Zhang, Y. 2009. Permafrost and climate change at Herschel Island (Qikiqtaruk), Yukon Territory, Canada. *Journal of Geophysical Research: Earth Surface* 114(F2): F02001.
<https://doi.org/10.1029/2008JF001087>
- . 2010. Sensitivity of active-layer development to winter conditions north of treeline, Mackenzie delta area, western Arctic coast. In: Kwok, C., Moorman, B., Armstrong, R., and Henderson, J., eds. *63rd Canadian Geotechnical Conference and 6th Canadian Permafrost Conference: Proceedings of a conference held 12–15 September in Calgary*. Paper 194. 1458–1465.
- Burn, C.R., Barrow, E., and Bonsal, B. 2004. Climate change scenarios for Mackenzie River valley. In: *57th Canadian Geotechnical Conference: Proceedings of a conference held 24–27 October in Québec City*. Session 7A. 2–8.
- Burn, C.R., Lewkowicz, A.G., and Wilson, M.A. 2021a. Long-term field measurements of climate-induced thaw subsidence above ice wedges on hillslopes, western Arctic Canada. *Permafrost and Periglacial Processes* 32(2):261–276.
<https://doi.org/10.1002/ppp.2113>
- Burn, C.R., Cooper, M., Morison, S.R., Pronk, T., and Calder, J.H. 2021b. The Canadian Federation of Earth Sciences scientific statement on climate change – its impacts in Canada, and the critical role of earth scientists in mitigation and adaptation. *Geoscience Canada* 48(2):59–72.
<https://doi.org/10.12789/geocanj.2021.48.173>
- Bush, E., and Lemmen, D.S. 2019. *Canada's changing climate report*. Ottawa: Government of Canada.
<https://doi.org/10.4095/314614>

- Canadian Standards Association. 2019. Technical guide: infrastructure in permafrost: A guideline for climate change adaptation. CSA PLUS 4011:19. Toronto: CSA Group.
- Environment and Climate Change Canada (ECCC). 2020. Canadian Climate Normals 1981–2010. Gatineau: ECCC.
https://climate.weather.gc.ca/climate_normals/index_e.html
- Fraser, R.H., Lantz, T.C., Olthof, I., Kokelj, S.V., and Sims, R.A. 2014. Warming-induced shrub expansion and lichen decline in the western Canadian Arctic. *Ecosystems* 17(7):1151–1168.
<https://doi.org/10.1007/s10021-014-9783-3>
- Hartmann, D.L., Klein Tank, A.M.G., Rusticucci, M., Alexander, L.V., Brönnimann, S., Charabi, Y.A.-R., Dentener, F.J., et al. 2013. Observations: Atmosphere and surface; Ch. 2 In: Stocker, T.F., Qin, D., Plattner, G.-K., Tignor, M., Allen, S.K., Boschung, J., Nauels, A., et al., eds. *Climate Change 2013: The Physical Science Basis. Contribution of Working Group I to the Fifth Assessment Report of the Intergovernmental Panel on Climate Change*. Cambridge: Cambridge University Press. Intergovernmental Panel on Climate Change (IPCC). 159–254.
<https://www.ipcc.ch/report/ar5/wg1/>
- Hayley, D.W., and Horne, B. 2008. Rationalizing climate change for design of structures on permafrost: a Canadian perspective. In: Kane, D.L., and Hinkel, K.M., eds. *Ninth International Conference on Permafrost: Proceedings of a conference held 29 June-3 July 2008 at the University of Alaska Fairbanks*. Vol. 1. 681–686.
- Hausfather, Z., Drake, H.F., Abbott, T., and Schmidt, G.A. 2020. Evaluating the performance of past climate model projections. *Geophysical Research Letters* 47(1): e2019GL085378.
<https://doi.org/10.1029/2019GL085378>
- Henn, B., Raleigh, M.S., Fisher, A., and Lundquist, J.D. 2013. A comparison of methods for filling gaps in hourly near-surface air temperature data. *Journal of Hydrometeorology* 14(3):929–945.
<https://doi.org/10.1175/JHM-D-12-027.1>
- Hjort, J., Karjalainen, O., Aalto, J., Westermann, S., Romanovsky, V.E., Nelson, F.E., Etzelmüller, B., and Luoto, M. 2018. Degrading permafrost puts Arctic infrastructure at risk by mid-century. *Nature Communications* 9: 5147.
<https://doi.org/10.1038/s41467-018-07557-4>
- Hjort, J., Streletskiy, D., Doré, G., Wu, Q., Bjella, K., and Luoto, M. 2022. Impacts of permafrost degradation on infrastructure. *Nature Reviews Earth & Environment* 3(1):24–38.
<https://doi.org/10.1038/s43017-021-00247-8>
- Intergovernmental Panel on Climate Change. 2000. *Emissions Scenarios*. [Nakicenovic N. and Swart, R. (Eds.)]. Cambridge: Cambridge University Press.
<https://www.ipcc.ch/report/emissions-scenarios/>
- . 2001. *Climate Change 2001: The Scientific Basis*. [Houghton, J.T., Ding, Y., Griggs, D.J., Noguera, M., van der Linden, P.J., Dai, X., Maskell, K., and Johnson, C.A. (Eds.)]. Cambridge: Cambridge University Press.
<https://www.ipcc.ch/report/ar3/wg1/>
- . 2013. *Climate Change 2013: The Physical Science Basis. Contribution of Working Group I to the Fifth Assessment Report of the Intergovernmental Panel on Climate Change* [Stocker, T.F., Qin, D., Plattner, G.-K., Tignor, M., Allen, S.K., Boschung, J., Nauels, A., Xia, Y., Bex, V., and Midgley, P.M. (eds.)]. Cambridge: Cambridge University Press.
<https://doi.org/10.1017/CBO9781107415324>
- . 2021a. *Climate Change 2021: The Physical Science Basis. Contribution of Working Group I to the Sixth Assessment Report of the Intergovernmental Panel on Climate Change* [Masson-Delmotte, V., Zhai, P., Pirani, A., Connors, S.L., Péan, C., Chen, Y., Goldfarb, L., et al. (eds.)]. Cambridge: Cambridge University Press.
<https://www.ipcc.ch/report/ar6/wg1/>
- . 2021b. Summary for Policymakers. In: *Climate Change 2021: The Physical Science Basis. Contribution of Working Group I to the Sixth Assessment Report of the Intergovernmental Panel on Climate Change* [Masson-Delmotte, V., Zhai, P., Pirani, A., Connors, S.L., Péan, C., Chen, Y., Goldfarb, L., et al. (eds.)]. Cambridge: Cambridge University Press. 3-32.
<https://www.ipcc.ch/report/ar6/wg1/chapter/summary-for-policymakers/>
- Kokelj, S.A., Beel, C.R., Connon, R.F., Graydon, C.E.D., Kokelj, S.V., and Burn, C.R. 2022. Peel Plateau climate data, Northwest Territories. Northwest Territories Geological Survey Report 2022-005.
<https://doi.org/10.46887/2022-005>
- Kokelj, S.V., Lantz, T.C., Tunnicliffe, J., Segal, R., and Lacelle, D. 2017. Climate-driven thaw of permafrost preserved glacial landscapes, northwestern Canada. *Geology* 45(4):371–374.
<https://doi.org/10.1130/G38626.1>
- Loranger Jr, B., Doré, G., Fortier, D., and Lemieux, C. 2015. Massive ice and ice-rich soil detection by gravimetric surveying at Dry Creek, southwestern Yukon Territory, Canada. In: Guthrie W.S., ed. *16th International Conference on Cold Regions Engineering: Proceedings of a conference held 19-22 July in Salt Lake City*. 46–56.
<https://doi.org/10.1061/9780784479315.005>

- Mark, D.M., and Church, M. 1977. On the misuse of regression in earth science. *Journal of the International Association for Mathematical Geology* 9(1):63–75.
<https://doi.org/10.1007/BF02312496>
- McCoy, V.M., and Burn, C.R. 2005. Potential alteration by climate change of the forest-fire regime in the boreal forest of central Yukon Territory. *Arctic* 58(3):276–285.
<https://doi.org/10.14430/arctic429>
- Mekis, É., and Vincent, L.A. 2011. An overview of the second generation adjusted daily precipitation dataset for trend analysis in Canada. *Atmosphere-Ocean* 49(2):163–177.
<https://doi.org/10.1080/07055900.2011.583910>
- Melvin, A.M., Larsen, P., Boehlert, B., Neumann, J.E., Chinowsky, P., Espinet, X., Martinich, J., et al. 2017. Climate change damages to Alaska public infrastructure and the economics of proactive adaptation. *Proceedings of the National Academy of Sciences* 114(2): E122–E131.
<https://doi.org/10.1073/pnas.1611056113>
- Miner, K.R., Turetsky, M.R., Malina, E., Bartsch, A., Tamminen, J., McGuire, A.D., Fix, A., Sweeney, C., Elder, C.D., and Miller, C.E. 2022. Permafrost carbon emissions in a changing Arctic. *Nature Reviews Earth & Environment* 3(1):55–67.
<https://doi.org/10.1038/s43017-021-00230-3>
- Porter, C., Morin, P., Howat, I., Noh, M-J., Bates, B., Peterman, K., Keeseey, S., et al. 2018, “ArcticDEM, Version 3”, Harvard Dataverse, V1, 20 June 2022.
<https://doi.org/10.7910/DVN/OHHUKH>
- Rantanen, M., Karpechko, A.Y., Lipponen, A., Nordling, K., Hyvärinen, O., Ruosteenoja, K., Vihma, T., and Laaksonen, A. 2022. The Arctic has warmed nearly four times faster than the globe since 1979. *Communications Earth & Environment* 3, 168.
<https://doi.org/10.1038/s43247-022-00498-3>
- Reimann, C., Filzmoser, P., Garrett, R.G., and Dutter, R. 2008. *Statistical data analysis explained: Applied environmental statistics with R*. Chichester: John Wiley & Sons.
<https://doi.org/10.1002/9780470987605>
- Schuur, E.A.G., McGuire, A.D., Schädel, C., Grosse, G., Harden, J.W., Hayes, D.J., Hugelius, G., et al. 2015. Climate change and the permafrost carbon feedback. *Nature* 520(7546):171–179.
<https://doi.org/10.1038/nature14338>
- Smith, M.W., and Riseborough, D.W. 2002. Climate and the limits of permafrost: a zonal analysis. *Permafrost and Periglacial Processes* 13(1):1–15.
<https://doi.org/10.1002/ppp.410>
- Smith, S.L., Throop, J., and Lewkowicz, A.G. 2012. Recent changes in climate and permafrost temperatures at forested and polar desert sites in northern Canada. *Canadian Journal of Earth Sciences* 49(8):914–924.
<https://doi.org/10.1139/e2012-019>
- Smith, S.L., O’Neill, H.B., Isaksen, K., Noetzi, J., and Romanovsky, V.E. 2022. The changing thermal state of permafrost. *Nature Reviews Earth & Environment* 3(1):10–23.
<https://doi.org/10.1038/s43017-021-00240-1>
- Standards Council of Canada, and Bureau de Normalisation du Québec. 2017. *Geotechnical Site Investigations for Building Foundations in Permafrost Zones*. CAN/BNQ 2501-500/2017. Ottawa: SCC Group.
https://www.bnq.qc.ca/images/pdf/Sommaire_SOD/SOD_2501-500_EN_2017.pdf
- Thienpont, J.R., Rühland, K.M., Pisaric, M.F.J., Kokelj, S.V., Kimpe, L.E., Blais, J.M., and Smol, J.P. 2013. Biological responses to permafrost thaw slumping in Canadian Arctic lakes. *Freshwater Biology* 58(2):337–353.
<https://doi.org/10.1111/fwb.12061>
- van Vuuren D.P., and Carter, T.R. 2014. Climate and socio-economic scenarios for climate change research and assessment: reconciling the new with the old. *Climatic Change* 122(3):415–429.
<https://doi.org/10.1007/s10584-013-0974-2>
- Vincent, L.A., Hartwell, M.M., and Wang, X.L. 2020. A third generation of homogenized temperature for trend analysis and monitoring changes in Canada’s climate. *Atmosphere-Ocean* 58(3):173–191.
<https://doi.org/10.1080/07055900.2020.1765728>
- Vincent, L.A., Zhang, X., Brown, R.D., Feng, Y., Mekis, É., Milewska, E.J., Wan, H., and Wang, X.L. 2015. Observed trends in Canada’s climate and influence of low-frequency variability modes. *Journal of Climate* 28(11):4545–4560.
<https://doi.org/10.1175/JCLI-D-14-00697.1>
- Vincent, L.A., Zhang, X., Mekis, É., Wan, H., and Bush, E.J. 2018. Changes in Canada’s climate: trends in indices based on daily temperature and precipitation data. *Atmosphere-Ocean* 56(5):332–349.
<https://doi.org/10.1080/07055900.2018.1514579>

- Wahl, H.E. Fraser, D.B., Harvey, R.C., and Maxwell, J.B. 1987. Climate of Yukon. Ottawa: Environment Canada, Atmospheric Environment Service.
<https://publications.gc.ca/site/eng/9.883308/publication.html>
- Wilcox, E.J., Keim, D., de Jong, T., Walker, B., Sonnentag, O., Sniderhan, A.E., Mann, P., and Marsh, P. 2019. Tundra shrub expansion may amplify permafrost thaw by advancing snowmelt timing. *Arctic Science* 5(4):202–217.
<https://doi.org/10.1139/as-2018-0028>
- Zhang, X., Flato, G., Kirchmeier-Young, M., Vincent, L., Wan, H., Wang, X., Rong, R., Fyfe, J., Li, G., and Kharin, V.V. 2019. Temperature and precipitation across Canada. In Bush, E. and Lemmen, D.S. eds. *Canada's changing climate report*. Ottawa: Government of Canada. 112–193.
<https://doi.org/10.4095/327811>
- Zhou, F., Zhang, A., and Hoeve, E. 2008. Cost impact of climate change-induced permafrost degradation on building foundations in Inuvik, Northwest Territories. In: Kane, D.L., and Hinkel, K.M., eds. *Ninth International Conference on Permafrost: Proceedings of a conference held 29 June-3 July 2008 at the University of Alaska Fairbanks*. Vol. 2. 2089–2094.